Polyethylene Based Ionomers as High Voltage Insulation Materials

Citation for the original published paper (version of record):
D'Auria, S., Pourrahimi, A., Favero, A. et al (2023). Polyethylene Based Ionomers as High Voltage Insulation Materials. Advanced Functional Materials, 33(36).
http://dx.doi.org/10.1002/adfm.202301878

ADVANCED FUNCTIONAL MATERIALS
www.afm-journal.de

Polyethylene Based Ionomers as High Voltage Insulation Materials

Silvia D'Auria, Amir Masoud Pourrahimi, Alessia Favero, Peter Neuteboom, Xiangdong Xu, Shuichi Haraguchi, Marko Bek, Roland Kádár, Enrico Dalcanale, Roberta Pinalli, Christian Müller,* and Jérôme Vachon**

Polyethylene based ionomers are demonstrated to feature a thermo-mechanical and dielectric property portfolio that is comparable to cross-linked polyethylene (XLPE), which may enable the design of more sustainable high voltage direct-current (HVDC) power cables, a crucial component of future electricity grids that seamlessly integrate renewable sources of energy. A new type of ionomer is obtained via high-pressure/high-temperature free radical copolymerization of ethylene in the presence of small amounts of ion-pair comonomers comprising amine terminated methacrylates and methacrylic acid. The synthesized ionomers feature a crystallinity, melting temperature, rubber plateau modulus and thermal conductivity like XLPE but remain melt-processable. Moreover, the preparation of the ionomers is free of byproducts, which readily yields a highly insulating material with a low dielectric loss tangent and a low direct-current (DC) electrical conductivity of 1 to $6{\cdot}10^{-14}$ S m^{-1} at 70 °C and an electric field of 30 kV mm^{-1}. Evidently, the investigated ionomers represent a promising alternative to XLPE-based high voltage insulation, which may permit to ease the production as well as end-of-use recycling of HVDC power cables by combining the advantages of thermoset and thermoplastic materials while avoiding the formation of byproducts.

1. Introduction

High voltage direct-current (HVDC) power cables are an integral part of modern electrical power grids that integrate renewable sources of energy.[1] The most advanced type of HVDC cable comprises an extruded insulation layer between the inner conductor and outer shielding, which allows the cable to be buried underground or placed at the bottom of the sea.[2] The most common insulation of extruded HVDC cables is composed of low-density polyethylene (LDPE), which is cross-linked with peroxides to form an infusible material that maintains dimensional stability above the melting temperature of LDPE, $T_m^{LDPE} \approx 110$ °C. Peroxide cross-linking, however, results in the formation of byproducts such as water, methane, cumyl alcohol and α-methyl styrene,[3] which represent a health hazard and cause premature aging of dielectrics under service conditions.[4] Hence, these byproducts must be removed from cross-linked polyethylene (XLPE), which can be achieved through a time and energy intensive degassing process.[4] Degassed XLPE features a low $\sigma_{DC} \approx 3{\cdot}10^{-14}$ S m^{-1} at an electric field of 30 kV mm^{-1} and 70 °C,[5] which is a typical HVDC cable operating temperature.

Alternative materials concepts that avoid the formation of byproducts during the cable manufacturing process, while maintaining the thermo-mechanical and dielectric properties of XLPE, are highly sought after.[6] The ability to dissipate the heat

S. D'Auria, A. Favero, E. Dalcanale, R. Pinalli
Department of Chemistry
Life Sciences and Environmental Sustainability
University of Parma and INSTM UDR Parma
43124, Parco Area delle Scienze 17/A Parma, Italy
E-mail: roberta.pinalli@unipr.it

The ORCID identification number(s) for the author(s) of this article can be found under https://doi.org/10.1002/adfm.202301878

DOI: 10.1002/adfm.202301878

S. D'Auria, P. Neuteboom, J. Vachon
SABIC Technology & Innovation
STC Geleen
6160 AH Geleen, The Netherlands
E-mail: jerome.vachon@sabic.com

A. M. Pourrahimi, A. Favero, S. Haraguchi, C. Müller
Department of Chemistry and Chemical Engineering
Chalmers University of Technology
41296 Göteborg, Sweden
E-mail: christian.muller@chalmers.se

X. Xu
Department of Electrical Engineering
Chalmers University of Technology
41296 Göteborg, Sweden

M. Bek, R. Kádár
Department of Industrial and Materials Science
Chalmers University of Technology
41296 Göteborg, Sweden

generated by the conducting core to avoid the risk of thermal runway and breakdown of the insulation material is another key parameter to be considered for high voltage insulation materials.[1]

Two types of strategies have been explored that either aim to replace peroxide curing or avoid cross-linking altogether. Byproduct free curing processes exploit click-chemistry type reactions between polyethylene copolymers, where permanent covalent bonds form upon the reaction of functional groups such as carboxylic acids and epoxides.[7,8] A second strategy is to use polypropylene copolymers or blends,[6,9–12] which thanks to the high melting temperature of polypropylene of up to $T_m^{PP} \approx 170$ °C maintain dimensional stability at elevated temperatures despite the absence of cross-links. Both types of blends feature electrical conductivities that are comparable to or even less than values reported for XLPE. The dielectric properties of novel insulation materials can be tuned further through the addition of metal oxide nanoparticles,[13,14] aromatic molecules[15,16] or organic semiconductors.[17,18] An additional advantage of thermoplastic formulations is the possibility to reprocess the material by remelting, which may ease recycling of the cable insulation for other applications once a cable has reached the end of its lifetime.

One approach that has not yet received much attention in the context of HVDC cable insulation is the use of dynamic bonds, presumably because of concerns that the introduction of additional chemical moieties may negatively affect the dielectric properties. One recent study[19] proposed the use of a dynamic network as a cable insulation material and explored the thermomechanical and dielectric properties of a polyethylene vitrimer comprising hydroxy ester cross-links formed through a byproduct free reaction of a dicarboxylic acid and epoxides that underwent transesterification in the presence of zinc acetate.[20,21] In terms of thermo-mechanical behavior, dynamic networks have the potential to combine the advantages of thermoset and thermoplastic insulation materials, i.e., an XLPE type rubber plateau above T_m^{PE}, as well as the possibility to reprocess the material at more elevated temperatures.

Here, we report the synthesis of a new type of polyethylene-based ionomer, where a few mole percent of positively and negatively charged groups are covalently bound to the polymer backbone. Amine terminated methacrylates and methacrylic acid, present in the form of ion pairs, are used as comonomers together with ethylene in a high-temperature/high-pressure process. The concept of having a direct copolymerization of ion-pair comonomers (IPCs) with non-charged monomers was first reported by Salomone et al.[22,23] and later extended to other charged monomers and types of polymerization, including atom transfer and free radical polymerization (ATRP, FRP) as well as reversible addition fragmentation chain transfer (RAFT).[24,25] However, these synthetic schemes are not suitable for ethylene, particularly when polymerized using metal-based catalysts that can be poisoned by charged molecules. We thus extend the IPC concept to polyethylene copolymers, which were obtained via high-pressure free radical copolymerization in the presence of ethylene and a suitable initiator.

The formation of ion pairs comprising an ammonium and a carboxylate group, which are both embedded within the polyethylene backbone, removes the need for labile counterions such as Na^+ or Zn^{2+} that are present in other types of ionomers such as ethylene-acrylate and ethylene-methacrylate copolymers.[26,27] This approach not only removes the need for an additional neutralization step after the synthesis but also results in materials that do not comprise any metal ions, which may become mobile at a sufficiently high electric field. Additionally, ethylene-acrylate and ethylene-methacrylate copolymers require the use of corrosion resistant processing equipment, i.e., both extruder and die should be made from corrosion resistant metals or must be nickel/chrome plated. Instead, IPC based materials do not require specialized equipment since the acid is fully neutralized by the amine counterpart. As a result, this type of ionomer features a low $\sigma_{DC} = 1$ to $6{\cdot}10^{-14}$ S m^{-1} at an electric field of 30 kV mm^{-1} and 70 °C, comparable to XLPE, together with a similar or even higher thermal conductivity $\kappa \geq 0.36$ W m^{-1} K^{-1}. Evidently, all-organic ionomers represent a new design strategy for high voltage insulation materials that combine the advantages of thermosets and thermoplastics while avoiding the formation of byproducts.

2. Results and Discussion

The one-step synthesis of polyethylene-based ionomers where both the cationic and anionic groups are covalently bound to the backbone is performed by directly reacting various IPCs with ethylene through a high-pressure/high-temperature free radical copolymerization.[28] This approach avoids the presence of mobile inorganic cations, which is the case for commercially available ionomers such as Surlyn (Dupont), a copolymer between ethylene and methacrylic acid whose synthesis requires a neutralization step,[29,30] and Dymalink (Total Cray Valley),[31] where zinc diacrylate is used as the cross-linker between two acidic groups. High-pressure/high-temperature free radical polymerization of ethylene leads to a branched chain configuration characteristic of low-density polyethylene (LDPE). The synthesis is compatible with a large range of comonomers with various functionalities that would not be feasible when using typical industrial Ziegler-Natta or metallocene catalysts where any "polar" moieties such as hydroxyl or amine groups would poison the catalyst.[32,33] Instead, by using free radical polymerization, it is possible to introduce such polar groups directly without any protecting group (**Figure 1**).

A wide range of IPCs were synthesized, either through an acid-base reaction, when secondary or tertiary amines were used, or through ion exchange metathesis in the case of primary amines used in the form of ammonium salts. IPCs based on secondary or tertiary amines were obtained by mixing the two starting reagents without the use of solvents (**Scheme 1**a). To realize IPCs based on primary amines, which are typically protonated (e.g. with HCl) to avoid transamidation reactions, co-dissolution of the two reagents in a mixture of methanol and dichloromethane and removal of the resulting insoluble inorganic salt to shift the equilibrium toward the product (Scheme 1b) was performed.

Structural variations of the starting monomers were devised to probe the influence of different ion pairs on the thermal, mechanical, and dielectric properties of the resulting copolymers. In particular, we used cationic comonomers with diverse degrees of alkylation of the amine moiety or different alkylating groups, while we exclusively used methacrylic acid for the anionic

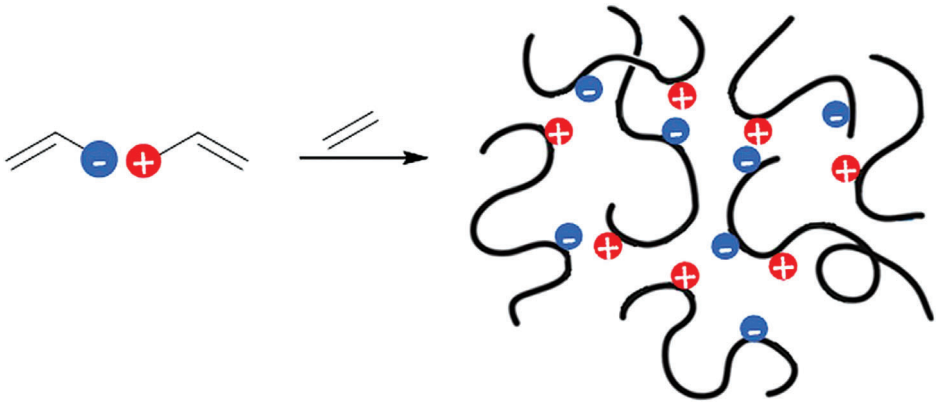

Figure 1. Schematic illustration of the ion-pair comonomer (IPC) concept.

comonomers (see **Figure 2**a, monomers M1-4). To confirm the formation of the ion pair, we used ^{1}H-NMR spectroscopy. An upfield shift of the vinyl protons belonging to the methacrylate unit is observed, while the ethane protons connecting the ester to the amine group and the methyl of the latter experience a downfield shift, as expected (Figures S1–S7, Supporting Information).

All ionomers (Figure 2c) were prepared through free radical polymerization by reacting the IPC and ethylene at a high pressure of ≈2000 bars and high temperature of 180 or 200 °C in an autoclave using a peroxide initiator (Figure 2b; see **Table 1** for reaction conditions). The IPCs were dissolved in methanol (50 wt%) and co-injected together with high-pressure ethylene in the autoclave through a static mixer. Methanol was chosen as a solvent since it does not have a large effect on the polymerization thanks to its very low chain transfer constant.

At the end of the reaction, the desired ionomers were recovered as a fine powder from the recuperation vessel and characterized through ^{1}H NMR spectroscopy (Figures S8–S15, Supporting Information), FTIR spectroscopy (Figure S16, Supporting Information), and elemental analysis. Elemental analysis indicates that the IPC content correlates with the comonomer content in the feed (Table 1). The ^{1}H NMR spectra of polymers P2-4 featured diagnostic peaks belonging to the amine moieties, as well as to the polyethylene backbone. The obtained polymers were quite pure, without the presence of any side product. On the contrary, for P1 the ^{1}H NMR spectrum indicated the presence of both unreacted monomers and side products, the latter due to unwanted amidation reactions (Figure S9, Supporting Information). We speculate that since M2-4 carry substituents on the amine group, amidation reactions are less likely to occur due to steric hindrance compared with M1. Moreover, the degree of conversion of M1 to P1 was found to be lower compared with M2-4 (Table S1, Supporting Information) and varied between different synthetic runs. Therefore, we decided to dismiss P1 during the remainder of this study.

The nitrogen content in the resulting polymers is a diagnostic measure of the presence of IPCs and allows their quantification. Therefore, elemental analysis was used to determine the IPC content, which was found to be ≈3 wt% for P2-4 and 4.5 wt% for P1. The calculated IPC content per 1000 carbons (-CH_2-) was similar for all synthesized ionomers, except P1 (see Table 1). Considering the low IPC content, we cannot be certain that every chain comprises both anions and cations and is independently neutral. Hence, we refer to the synthesized materials as *ionomers*, and not *zwitterionic polymers*, which, arguably, is a good description for most polymer chains.

We confirmed that both the synthesized ionomers as well as melt-pressed films could be dissolved in *p*-xylene at 100 °C, which suggests that the material does not form one inseparable network (Figure S17, Supporting Information). Size exclusion chromatography (SEC) of the ionomers using 1,2-dichlorobenzene as the solvent indicated the presence of aggregates with apparent molecular weights of more than 10^6 g mol^{-1} (not shown), which

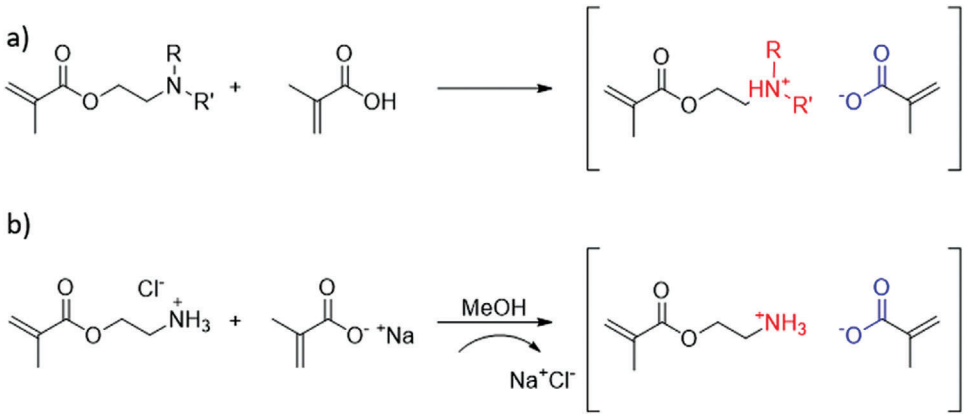

Scheme 1. a) Acid-base reaction in the case of secondary and tertiary amines and b) exchange metathesis reaction in the case of a primary amine.

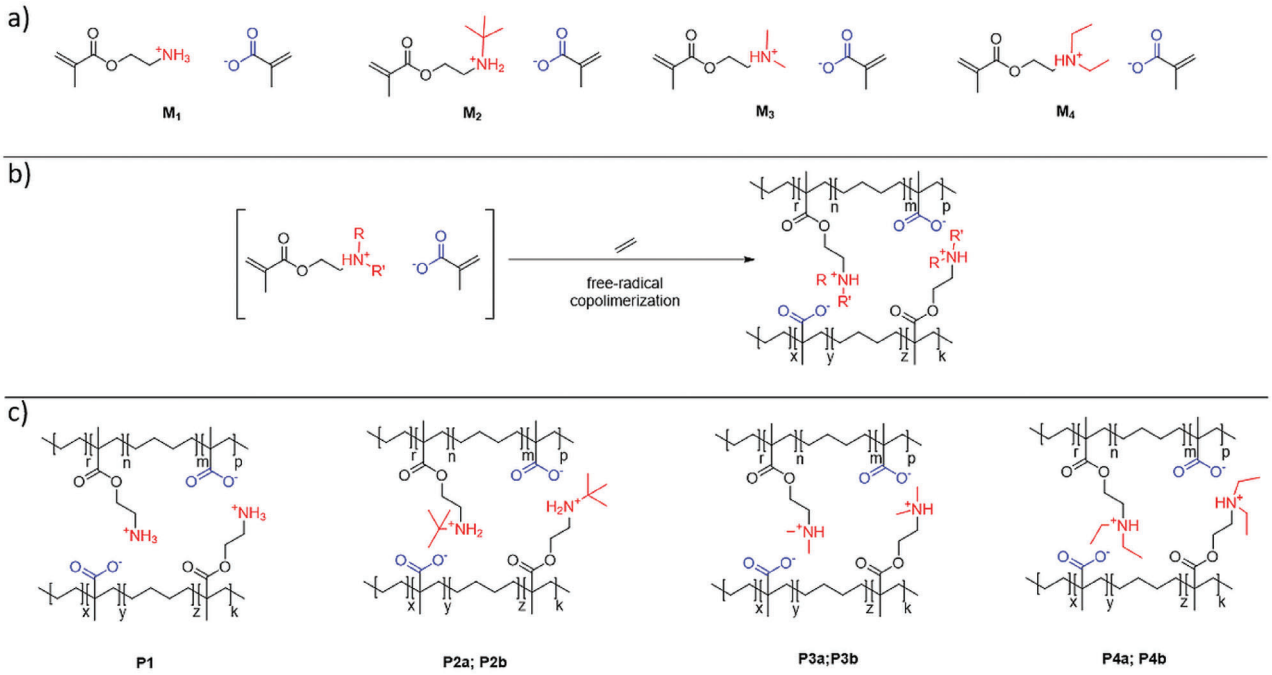

Figure 2. a) The synthetized ion pair comonomers (IPCs), b) free radical polymerization reaction, and c) corresponding ionomers; the letters a and b identify ionomers polymerized at 180 and 200 °C, respectively (see Table 1).

likely consist of several polyethylene backbones linked via ion pairs. We argue that the ionomers should not be thought of as individual macromolecules but rather clusters of macromolecules whose makeup can evolve due to exchangereactions between different ion pairs.

Differential Scanning Calorimetry (DSC) was performed to gain further insight into the microstructure of the synthesized ionomers and to assess their thermal properties. Second heating thermograms of all ionomers feature a similar crystallinity of ≈40% and a peak melting temperature T_m = 113 to 114 °C, slightly higher than reference LDPE (Table 2 and Figure S18, Supporting Information), indicating that the IPCs do not significantly affect the microstructure of the polymer matrix. We also note that all DSC thermograms feature a single melting endotherm, which is consistent with a relatively even distribution of the comonomers along the polymer backbone.

We used the Gibbs-Thomson equation to calculate the peak lamellar thickness:

$$l_c = \frac{2\sigma_e}{\rho \cdot \Delta H_f^0} \cdot \frac{T_m^0}{T_m^0 - T_m} \quad (1)$$

where $\sigma_e = 90.4$ mJ m^{-2} is the surface energy for polyethylene, $\rho = 1$ g cm^{-3} is the density of the crystal phase, $\Delta H_f^0 = 286.2$ J g^{-1} is the heat of fusion, and $T_m^0 = 418.6$ K is the equilibrium melting temperature of polyethylene. We obtained values of l_c ranging from 8.1 to 8.4 nm, which are higher compared with the values obtained for the LDPE and XLPE reference materials (Table S2, Supporting Information), likely because of differences in the degree of long-chain branching.

Dynamic mechanical thermal analysis (DMTA) in tensile mode was used to analyze the thermo-mechanical properties

Table 1. IPC molecular weight M_{IPC}, IPC content in the feed and temperature T used for free radical polymerization of ionomers, IPC content of the synthesized ionomers from elemental analysis of the nitrogen content given in wt%, mol% and per 1000 CH_2.

IPC	M_{IPC} [g mol^{-1}]	IPC feed [mol%]	T [°C]	Ionomer	IPC content [wt%]	IPC content [mol%]	IPC content per 1000 CH_2
M1	215.25	0.1	200	P1	4.5	0.61	3.1
M2	271.35	0.05	180	P2a	3.1	0.33	1.7
			200	P2b	2.9	0.31	1.5
M3	243.30	0.05	180	P3a	2.9	0.34	1.7
			200	P3b	2.8	0.33	1.7
M4	271.35	0.05	180	P4a	2.9	0.31	1.5
			200	P4b	2.9	0.31	1.5

Table 2. Peak melting temperature T_m and crystallinity $X_c = \Delta H_f / \Delta H_f^0$ from DSC, where ΔH_f is the melting enthalpy and $\Delta H_f^0 = 286.2$ J g^{-1}, storage modulus E' at 150 °C from DMTA, molecular weight between cross-links M_c according to Equation 2, number of crosslinks N_c per 1000 CH_2, thermal conductivity κ at room temperature, electrical conductivity σ_{DC} at 70 °C and an electric field of 30 kV mm^{-1} of LDPE, degassed XLPE, Surlyn as well as the synthesized ionomers; the error in σ_{DC} is estimated to be 30%.[12]

Material	T_m [°C]	X_c [%]	E' at 150 °C [MPa]	M_c [kg mol^{-1}]	N_c per 1000 CH_2	κ at r. t. [W m^{-1} K^{-1}]	σ_{DC} at 70 °C [10^{-14} S m^{-1}]
LDPE	110	39	–	–	–	0.41 ± 0.08	7.0 ± 2.1
XLPE	108	42	3.7	2.3	6.2	0.36 ± 0.004	4.5 ± 1.4
Surlyn	90	10	–	–	–	0.29 ± 0.002	3.4 ± 1.0
P2a	114	40	0.8	10.8	1.3	0.39 ± 0.006	1.0 ± 0.3
P2b	113	41	1.01	8.2	1.7	0.38 ± 0.006	6.0 ± 1.8
P3a	114	42	2.6	3.2	4.4	0.37 ± 0.001	3.1 ± 0.9
P3b	113	41	1.14	7.3	1.9	0.35 ± 0.006	5.3 ± 1.6
P4a	114	39	1.4	6.0	2.3	0.39 ± 0.001	1.6 ± 0.5
P4b	113	42	0.85	9.8	1.4	0.36 ± 0.009	1.7 ± 0.5

of melt-pressed films of the ionomers up to 200 °C (thermal gravimetric analysis (TGA) shows no weight loss up to 200 °C, see Figures S19-S24 Supporting Information). All materials display a storage modulus E' between 200 and 500 MPa at room temperature (**Figure 3**). DMTA thermograms of reference LDPE and Surlyn feature a significant decrease in E' above their melting temperature(s), resulting in a molten material above 120 °C (Figure 3). In contrast, XLPE (see experimental section for details) with a gel content of 68% gave rise to a rubber plateau above its T_m = 108 °C with a value of $E' \approx 3.7$ MPa at 150 °C (Table 2). Likewise, DMTA thermograms of the synthesized ionomers feature a distinct rubber plateau above T_m^{PE}, confirming that the introduction of IPCs leads to the formation of a network (Figure 3a and b). Except for P2a, the moduli of the polymers synthesized at 200 °C are lower compared with the modulus of the corresponding polymers synthesized at 180 °C. P3a exhibits a rubber plateau modulus of $E' \approx 2.6$ MPa at 150 °C (Table 2), which is like the value obtained for XLPE. The molecular weight between consecutive crosslinks M_C was estimated according to equation 2:

$$M_c = \frac{\rho RT}{G'} \quad (2)$$

Where $\rho = 0.790$ g cm^{-3} is the density at temperature T = 150 °C (423 K), R the universal gas constant and $G' = E' / [2(1+\upsilon)] = E' / 3$ the shear modulus at T = 150 °C assuming a Poisson's ratio $\upsilon = 0.5$. The number of network points N_c per 1000 carbons (−CH_2−) was then estimated by dividing 14 kg mol^{-1} with M_c (Table 2). For XLPE we obtain a value of $M_c \approx 2.3$ kg mol^{-1}, which corresponds to $N_c \approx 6.3$ per 1000 carbons. Ionomer P3a yields similar values of $M_c \approx 3.2$ kg mol^{-1} and $N_c \approx 4.4$ per 1000 carbons (Table 2), which suggests that the amount of comonomer and type of amine group can be selected to match the thermo-mechanical properties of XLPE. In general, for P2-4 the estimated value for N_c is comparable to or larger than the number of IPCs per 1000 carbons (cf. Tables 1 and 2), which suggests that the majority of IPCs, in addition to long-chain branches and trapped entanglements, form a network point. The overall picture emerging from these data is the presence of ionic network points that reinforce the molten ionomers.

In a further set of experiments dynamic oscillatory shear and extensional rheology measurements were carried out to gain further insights into the viscoelastic properties of the ionomer melts. Dynamic oscillatory shear measurements at 150 °C of LDPE and Surlyn reveal a crossover frequency where the shear storage and

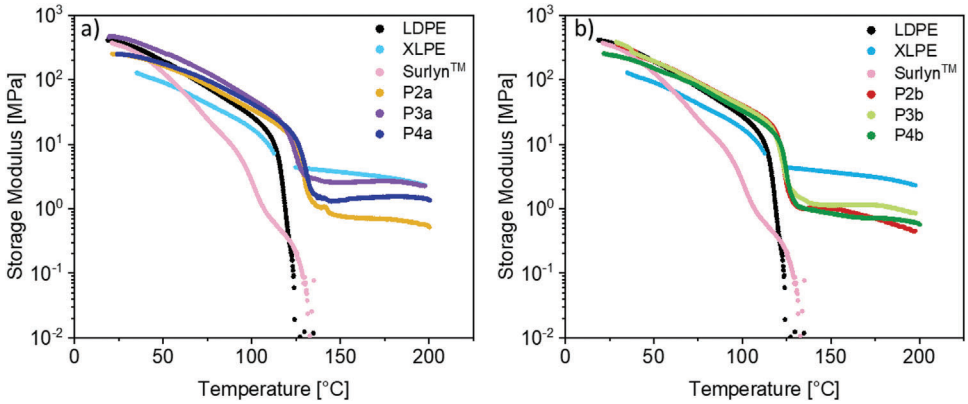

Figure 3. DMTA thermograms of: a) LDPE, XLPE, Surlyn, P2-4a and b) LDPE, XLPE, Surlyn, P2-4b.

loss modulus are of equal magnitude, i.e., $G' = G''$, indicating a transition from an elastic- to a viscous-dominated behavior with decreasing frequency (Figure S25). The longest relaxation time of the polymer melt $\tau_d = 1/\omega_{G'=G''}$ was found to be 5.6 s for LDPE and 0.7 s for Surlyn. In contrast, XLPE shows an elastic-dominated behavior in the entire tested frequency range from $\omega = 0.01$ to 600 rad s^{-1}, i.e., $G' > G''$ as expected for a cross-linked polymer. Likewise, the ionomers P2-4a,b have virtually identical viscosity functions compared to XLPE both in terms of magnitude and shear thinning slope, retaining their elastic network character across the tested frequency range, in agreement with the DMTA measurements (see Figure 3). For all ionomers but P3a we observe that the difference between G' and G'' decreases at lower frequencies, and thus a crossover point may exist at $\omega << 0.01$ rad s^{-1} where $G' = G''$ implying longest relaxation times of $\tau_d >> 600$ s (Figure S25, Supporting Information).

Extensional rheology measurements allowed us to monitor the transient uniaxial extensional viscosity as a function of Hencky strain rate from $\dot{\varepsilon} = 10^{-2}$ to 10^{1} s^{-1} (Figure S26, Supporting Information). LDPE displays significant strain hardening, as expected due to its long-chain branched molecular topology. A similar degree of strain hardening is observed in the case of XLPE as well as the ionomers P3a,b and P4a,b indicating that strain stretching occurs between the covalent network points in case of XLPE and ionic network points in case of the ionomers. In contrast, the ionomers P2a,b with a *tert*-butyl group on the secondary amine feature minimal strain hardening. Since these two materials feature a similar N_c as, e.g., P3b and P4b (see Table 2), we argue that chain stretching between cross-links and thus strain hardening is absent because the ionic network points are able to reorganize to a greater extent. This observation is consistent with a lower dissociation energy of ion-pairs due to the presence of a bulky alkyl group at the ammonium cation, which increases the anion/cation distance.[34–36]

The transient plane source method was used to determine the thermal diffusivity α and heat capacity C_p at room temperature (Table S3), and the thermal conductivity was calculated according to:

$$\kappa = \alpha \rho C_p \tag{3}$$

using a density of $\rho = 0.921$ g cm^{-3}. We find that LDPE has a thermal conductivity at room temperature of $\kappa = 0.41$ W m^{-1} K^{-1} while XLPE shows a lower value of $\kappa = 0.36$ W m^{-1} K^{-1} (Table 2). Surlyn features a significantly lower thermal conductivity, which we assign to the lower crystallinity of the material. Ionomers P2-4 display slightly larger values than XLPE, e.g., $\kappa = 0.39$ W m^{-1} K^{-1} for P4a, which we explain with a similar crystallinity, but slightly larger lamellar thickness as indicated by the larger T_m compared with XLPE (see Table S2, Supporting Information).

In a further set of experiments, we determined the electrical conductivity of the ionomers. Films with thicknesses of 0.14 to 0.16 mm were placed between two planar electrodes, with the measuring electrode surrounded by a shielding electrode, and the electrode system was placed in an oven to maintain a temperature of 70 °C (**Figure 4**a). We applied a DC voltage for 18 h that gave rise to an electric field of 30 kV mm^{-1}, followed by an intermittent interval during which the applied voltage was turned off for 6 h to simulate a discharging event, and finally the same DC voltage was reapplied for another 18 h. After reapplication of the voltage the leakage currents and hence the apparent conductivity rapidly approached quasi steady–state behavior, indicating that polarization did not significantly affect the materials (Figure 4; Figure S27, Supporting Information). The apparent conductivity gradually decayed, approaching quasi steady–state conditions at

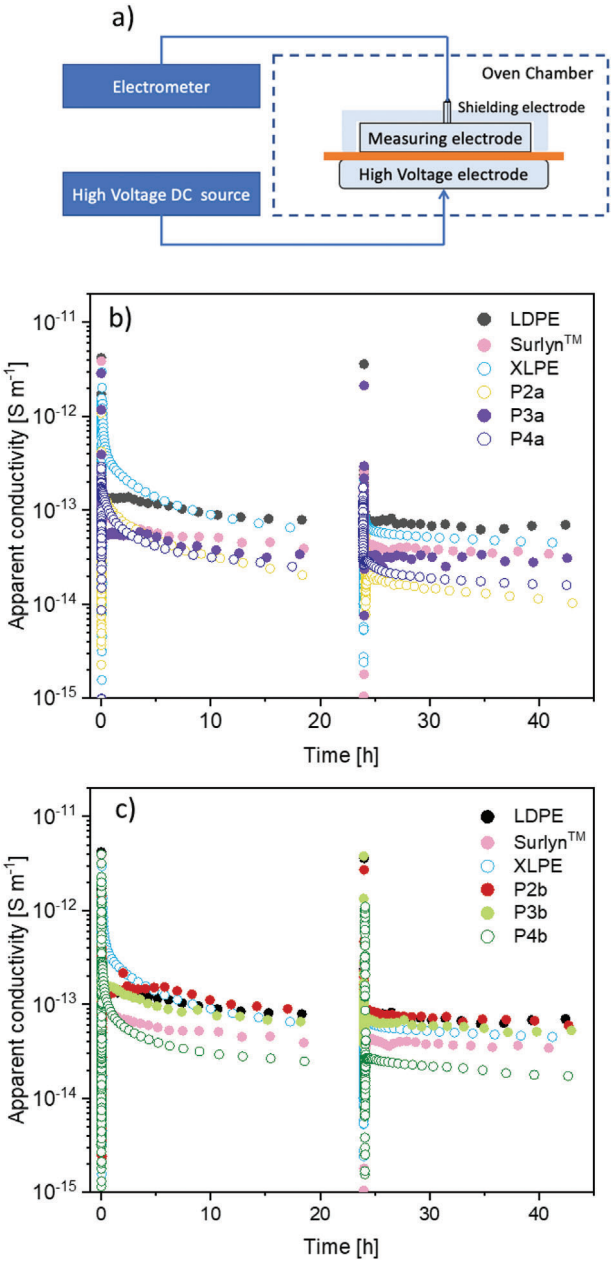

Figure 4. a) Schematic of the setup used for leakage current measurements, and apparent conductivity $\sigma = IV^{-1} \cdot 4L(\pi D^2)^{-1}$ where L is the distance between the measuring and high voltage electrode (i.e., the sample thickness), D the diameter of the measuring electrode, V the applied voltage and I the leakage current recorded at 70 °C and 30 kV mm^{-1} with an intermittent step of 6 h during which the applied voltage was turned off for b) LDPE, XLPE, Surlyn and ionomers P2-4a and c) LDPE, XLPE, Surlyn and ionomers P2-4b. Open symbols: $D = 28$ mm; closed symbols: $D = 59$ mm.

the end of the measurement, and the value obtained at the end of the second 18 h period was used as an estimate for σ_{DC}. While the leakage current can decrease further when measuring insulation materials over longer periods of time,[37] we note that for some of the materials the here recorded values appear to decrease less rapidly toward the end of the measurement (see Figure S27, Supporting Information for log-log plot of apparent conductivity versus time). For LDPE and XLPE we obtained values of $\sigma_{DC} = 7.0$ and $4.5{\cdot}10^{-14}$ S m^{-1}, respectively (Table 2), the latter being similar to values reported for XLPE used for high voltage insulation.[8] Remarkably, despite the presence of polar functional groups, ionomers P2-4a synthesized at 180 °C feature a low $\sigma_{DC} = 1$ to $3.1{\cdot}10^{-14}$ S m^{-1}, which is close to the value obtained for XLPE. Instead, P2-4b, which were synthesized at 200 °C, display slightly higher values of $\sigma_{DC} = 1.7$ to $6{\cdot}10^{-14}$ S m^{-1}.

To rule out that σ_{DC} unduly increases at higher temperatures we also carried out measurements at 30 kV mm^{-1} and 90 °C, albeit for a period of only 3 h to minimize the risk of breakdown. For P3a, for instance, we observe that σ_{DC} is five-fold higher at 90 °C compared to 70 °C (Figure S28, Supporting Information), an increase that is expected given the temperature-dependence of charge conduction in high voltage insulation materials.[38,39]

Evidently, the selection of a judicious amount of IPCs in combination with tuning of the polymerization conditions results in materials that display a promising combination of thermo-mechanical and dielectric properties. The ionomers P2a and P4a, for example, offer a desirable combination of a low $\sigma_{DC} < 2{\cdot}10^{-14}$ S m^{-1} but high $\kappa = 0.39$ W m^{-1} K^{-1}, while the tensile storage modulus at 150 °C ranges from $E' \approx 0.8$ to 1.4 MPa, slightly less than reference XLPE (Table 2). Thermal aging of LDPE leads to the formation of carbonyl groups that can act as traps for charge carriers, leading to a reduction in σ_{DC} with a minimum value for a certain degree of oxidation.[40,41] Likewise, it can be anticipated that there is an IPC content for which optimal electrical properties are obtained.

Finally, we carried out dielectric frequency response spectroscopy at 70 and 90 °C across a frequency range of 0.01 to 1000 Hz and determined the dielectric loss tangent tan δ. Both LDPE and Surlyn feature a low value of tan $\delta = 0.0021$ and 0.0032 at 70 °C and 0.01 Hz (Figure S29 and Table S4, Supporting Information),[5] where tan δ is dominated by DC conduction losses, which must be low to enable the design of HVDC cable insulation. At higher frequencies, e.g., 50 Hz, the alternating current (AC) frequency used in Europe, LDPE displays an even lower tan $\delta = 0.0003$ while Surlyn shows a much higher value of 0.0047. Gratifyingly, several ionomers feature a loss tangent that is comparable to values measured for LDPE, e.g., 0.0015 and 0.0004 in case of P2a at 0.01 and 50 Hz, respectively (Table S4, Supporting Information), which suggests that the investigated ionomers give rise to minimal dielectric loss despite the presence of carboxylate:ammonium ion pairs.

3. Conclusions

In this work, we introduce polyethylene-based ionomers as potential insulation materials for high voltage power cables. The studied ionomers were synthesized via high-pressure/high-temperature free radical copolymerization in the presence of a suitable initiator by directly reacting various ion-pair comonomers (IPCs) with ethylene. The IPCs comprise amino terminated methacrylates and methacrylic acid that differ in the type and number of substituents on the amine group. This approach resulted in melt-processable materials with thermo-mechanical properties like XLPE, while avoiding the presence of mobile inorganic cations or cross-linking side products that can affect the dielectric properties. The synthesized ionomers exhibit a melting temperature and crystallinity like XLPE and LDPE, indicating that the IPCs do not significantly affect the microstructure of the polymer matrix. Dynamic mechanical thermal analysis (DMTA) indicated that all investigated ionomers feature a rubber plateau above their melting temperature, like XLPE. Despite the presence of ionic moieties, the obtained ionomers display promising insulating properties, as evidenced by a low dielectric loss tangent and low electrical conductivity of $\sigma_{DC} = 1$ to $6{\cdot}10^{-14}$ S m^{-1} at 70 °C and an electric field of 30 kV mm^{-1}, comparable to or lower than the value measured for XLPE, $\sigma_{DC} = 4.5{\cdot}10^{-14}$ S m^{-1}, the most common insulation material used for extruded high voltage cables. Moreover, the ionomers exhibit a relatively high thermal conductivity $\kappa = 0.35$ to 0.39 W m^{-1} K^{-1} comparable to or larger than XLPE ($\kappa = 0.36$ W m^{-1} K^{-1}). Importantly, properties like the elastic modulus at elevated temperatures as well as the electrical and thermal conductivity can be tuned by a judicious selection of the amine group of the IPC, which offers the opportunity to optimize the ionomer concept for specific application requirements. Overall, the investigated type of ionomers show potential as a viable alternative to XLPE for high voltage power cable insulation.

4. Experimental Section

Materials: Ionomers P1-4a,b were synthesized by free radical polymerization of ethylene in the presence of the IPCs M1-4 (see Table 1 and Supporting Information for details). LDPE with a melt flow rate (MFR) of 0.85 g / 10 min (190 °C; 2.16 kg) and density of 0.921 g cm^{-3} was obtained from SABIC. An ethylene-methacrylic acid ionomer neutralized with NaOH Surlyn (14.5 wt% of MAA and 2.02 wt% of Na^+) was obtained from Dow. Unless otherwise specified, solvents and chemicals used for the synthesis of the IPCs M1-4 and all the ionomers were purchased from Sigma–Aldrich and used as received. All solvents employed were laboratory grade and used as received.

Sample Preparation: Samples for DMTA and DC conductivity measurements were prepared by melt-pressing the ionomers or LDPE at 150 °C, including a 5 min melting step followed by application of 150 kN for 10 min. Some melt-pressed ionomer films contained physical impurities that were removed by cutting followed by melt-pressing of the remaining material for a second time. To prepare XLPE, milled LDPE was dispersed in a solution of dicumyl peroxide (DCP) in methanol at 40 °C and stirred for 1 h, followed by solvent evaporation. The resulting milled LDPE infused with 1 wt% DCP was melt-pressed at 120 °C for 5 min. The temperature was then increased to 180 °C, where the sample was allowed to cross-link for 10 min before cooling. Finally, XLPE samples were degassed in a vacuum oven at 40 °C. The gel content was measured by submerging 150 mg of material in 500 mL of decalin for 20 h followed by drying and weighing of the insoluble fraction.

Nuclear Magnetic Resonance Spectroscopy: Nuclear magnetic resonance (NMR) spectra were recorded using a Bruker AVANCE 400 (400 MHz) spectrometer at room temperature. Chemical shifts were reported in parts per million (ppm). ^{1}H-NMR chemical shifts were given in reference to the residual solvent peak at 7.26 ppm in $CDCl_3$, at 6.00 ppm for tetrachloroethane-d_2 (TCE-d_2), and at 2.50 ppm in dimethyl sulfoxide-d_6 (DMSO-d_6). High-temperature NMR spectra were recorded on a Bruker

AVANCE III (500 MHz) equipped with a cryogenically cooled probe head at 80 or 120 °C in TCE-d_2.

Elemental Analysis: Elemental analysis (EA) was carried out with a CHNS Thermo Fisher FlashSmart instrument. Samples were burned in the presence of oxygen. The nitrogen content was determined by means of thermal conductivity (TC) and volumetric analysis.

Fourier Transform Infrared Spectroscopy: Fourier transform infrared spectroscopy (FTIR) in attenuated total reflectance (ATR) mode was performed on powder samples with a Perkin Elmer FTIR Spectrum Two instrument equipped with a GladiATR attachment from Pike Technologies. The background was subtracted from every recorded spectrum.

Thermogravimetric Analysis: Thermogravimetric analysis (TGA) was performed under nitrogen atmosphere using a Perkin Elmer TGA 8000. Samples were heated to 800 °C at a heating rate of 10 °C min^{-1}.

Differential Scanning Calorimetry: Differential scanning calorimetry (DSC) measurements were carried out under nitrogen between −50 and 150 °C at a scan rate of 10 °C min^{-1}, using a Mettler Toledo DSC2 calorimeter. The sample weight was 5–10 mg.

Dynamic Mechanical Thermal Analysis: Dynamic mechanical thermal analysis (DMTA) was carried out in tensile mode using a TA Q800 DMA in tensile mode on 30 mm × 11 mm pieces cut from 0.7 mm thick melt-pressed films. Variable-temperature measurements from 25 to 200 °C were done at a heating rate of 3 °C min^{-1}, with a preload force of 0.01 N, a maximum strain of 0.05% and a frequency of 1 Hz.

Rheology: Rheological properties in simple shear and uniaxial extension were determined using an Anton Paar MCR702e Space rheometer equipped with a convection oven for temperature control. All tests were performed at 150 °C. Shear rheological properties were measured in oscillatory shear using an 8 mm plate-plate measuring geometry (and 15 mm plate-plate geometry for LDPE and Surlyn) in counter-oscillation separate motor-transducer configuration. The angular frequency was varied from 0.01 to 600 rad s^{-1} at shear strain amplitudes adjusted between 0.03%–0.3% to contain the measurements within the linear viscoelastic regime. Oscillatory shear measurements were performed in a nitrogen atmosphere. The extensional rheological properties were measured using an extensional fixture for rotational rheometry in separate motor-transduced configuration. Thus, the transient uniaxial extensional viscosity, $\eta_E^+(t, \dot{\varepsilon})$, was recorded at four Hencky strain rates,[42] $\dot{\varepsilon} = 10^{-2}$, 10^{-1}, 10^0, 10^1 s^{-1} at 150 °C.

Thermal Conductivity Measurements: The thermal diffusivity and heat capacity were measured with a TPS 2500 S instrument from Hot Disk at room temperature. A 7854 Kapton sensor was sandwiched between two 4.6-mm-thick specimen films with a diameter of 3.0 mm, fixed between two steel blocks. During each measurement, 4 mW of heating power was supplied over 2 s, resulting in a probing depth of ≈2 mm.

DC Conductivity Measurements: The test cell consisted of a three-electrode setup that was placed in an oven and connected to a high-voltage power supply (Keithley 2290). The high voltage electrode had a diameter of 60 mm; a measuring electrode with a diameter of $D = 28$ or 59 mm was used, as indicated. A DC voltage of $V = 4.2$ to 4.8 kV was applied across $L = 0.14$ to 0.16 mm thick films. To ensure good surface contact between the specimen and electrodes, a 0.7 mm thick electrically conductive rubber layer was applied on all three electrode contact surfaces. The volume leakage current was recorded with a Keithley 6517B electrometer, and dynamically averaged. Measurements at 70 °C were carried out by applying an electric field of 30 kV mm^{-1} for ≈18 h, then the voltage was switched-off for ≈6 and finally the same electric field was reapplied for another 18 h (Figure 4; Figure S27, Supporting Information). σ_{DC} at 70 °C was calculated based on the charging currents obtained at the end of the second 18 h period (Table 2). Alternatively, for measurements at 90 °C the rubber layers were removed resulting in direct surface contact between the specimen and electrodes; an electric field of 30 kV mm^{-1} was applied for 3 h and σ_{DC} was calculated based on the charging current at the end of the measurement (Figure S28, Supporting Information).

Dielectric Frequency Response Measurements: A Megger IDAX 300 insulation diagnostic analyzer was used to obtain the loss factor of 0.14 to 0.16 mm thick films. The test cell consisted of a three-electrode setup (see Figure S29, Supporting Information) that was placed in an oven at 70 or 90 °C for 5 h prior to the measurement to allow the temperature to stabilize. The measuring electrode with a diameter of $D = 59$ mm was fully covered by a guard electrode with a gap distance of 0.1 mm to minimize electrode edge effects. The voltage electrode on the other side of the films covered both electrodes. An rms voltage of 140 V was applied and the frequency was varied from 0.01 to 1000 Hz.

Supporting Information

Supporting Information is available from the Wiley Online Library or from the author.

Acknowledgements

C.M., S.H. and A.M.P. gratefully acknowledge the Swedish Foundation for Strategic Research (grant no. FFL15-0147), the Swedish Research Council Formas (grant no. 2018-00886) and the Chalmers Area of Advance Production for financial support. A.F. acknowledges the Fondazione CRUI (project PILOT) for financial support of her fellowship. S.D., R.P., C.M. and E.D. acknowledge the project VIT, funded through the European Union Horizon 2020 Program (H2020-MSCA-RISE-2020 under grant agreement no. 101008237). This work benefited from the equipment and framework of the COMP-HUB Initiative, funded by the Departments of Excellence program of the Italian Ministry for Education, University and Research (MIUR, 2018–2022).

Conflict of Interest

The authors declare no conflict of interest.

Data Availability Statement

The data that support the findings of this study are available from the corresponding author upon reasonable request.

Keywords

cross-linked polyethylene, electrical insulators, HVDC power cables, ionomers, thermal conductivity

Received: March 31, 2023
Published online:

[1] G. C. Montanari, P. H. F. Morshuis, M. Zhou, G. C. Stevens, A. S. Vaughan, Z. Han, D. Li, *High Volt.* **2018**, *3*, 90.
[2] G. Mazzanti, M. Marzinotto, *Extruded Cables for High-Voltage Direct-Current Transmission*, Wiley, New Jersey, **2013**.
[3] T. H. A. Smedberg, B. Gustafsson, *Polymer* **1997**, *38*, 4127.
[4] T. Andrews, R. N. Hampton, A. Smedberg, D. Wald, V. Waschk, W. Weissenberg, *IEEE Electr. Insul. Mag.* **2006**, *22*, 5.
[5] S. Kumara, X. D. Xu, T. Hammarström, Y. W. Ouyang, A. M. Pourrahimi, C. Müller, Y. V. Serdyuk, *Energies* **2020**, *13*, 1434.
[6] T. Andritsch, A. Vaughan, G. C. Stevens, *IEEE Electr. Insul. Mag.* **2017**, *33*, 27.
[7] M. Mauri, A. Peterson, A. Senol, K. Elamin, A. Gitsas, T. Hjertberg, A. Matic, T. Gkourmpis, O. Prieto, C. Müller, *J. Mater. Chem. C* **2018**, *6*, 11292.
[8] M. Mauri, A. I. Hofmann, D. Gomez-Heincke, S. Kumara, A. M. Pourrahimi, Y. W. Ouyang, P. O. Hagstrand, T. Gkourmpis, X. D. Xu, O. Prieto, C. Müller, *Polym. Int.* **2020**, *69*, 404.

[9] C. D. Green, A. S. Vaughan, G. C. Stevens, A. Pye, S. J. Sutton, T. Geussens, M. J. Fairhurst, *IEEE Trans. Dielectr. Electr. Insul.* **2015**, *22*, 639.
[10] X. Y. Huang, Y. Y. Fan, J. Zhang, P. K. Jiang, *IEEE Trans. Dielectr. Electr. Insul.* **2017**, *24*, 1446.
[11] S. Yu, S. H. Lee, J. A. Han, M. S. Ahn, H. Park, S. W. Han, D. H. Lee, *Polymer* **2020**, *202*, 122674.
[12] Y. W. Ouyang, A. M. Pourrahimi, I. Östergren, M. Mellqvist, J. Anevall, A. Soroudi, A. Lund, X. D. Xu, T. Gkourmpis, P. O. Hagstrand, C. Müller, *High Volt.* **2022**, *7*, 251.
[13] A. M. Pourrahimi, R. T. Olsson, M. S. Hedenqvist, *Adv. Mater.* **2018**, *30*, 1703624.
[14] A. Soroudi, Y. W. Ouyang, F. Nilsson, I. Östergren, X. D. Xu, Z. R. Li, A. M. Pourrahimi, M. Hedenqvist, T. Gkourmpis, P. O. Hagstrand, C. Müller, *Nanoscale* **2022**, *14*, 7927.
[15] Z. J. Wei, H. Y. Liu, L. W. Yu, S. W. Xiao, Y. X. Hou, X. R. Chen, *J. Appl. Polym. Sci.* **2020**, *137*, 49185.
[16] X. R. Chen, A. Paramane, H. Y. Liu, J. Tie, Z. J. Wei, Y. Tanaka, *Polym. Eng. Sci.* **2020**, *60*, 717.
[17] A. M. Pourrahimi, S. Kumara, F. Palmieri, L. Y. Yu, A. Lund, T. Hammarström, P. O. Hagstrand, I. G. Scheblykin, D. Fabiani, X. D. Xu, C. Müller, *Adv. Mater.* **2021**, *33*, 2100714.
[18] B. Dang, J. Hu, Y. Zhou, J. L. He, *J Phys D Appl Phys* **2017**, *50*, 455303.
[19] Y. Zhao, H. Mao, T. Zhang, Z. Guo, D. Bai, H. Bai, Q. Zhang, H. Xiu, F. Q, *Ind. Eng. Chem. Res.* **2022**, *61*, 13126.
[20] D. Montarnal, M. Capelot, F. Tournilhac, L. Leibler, *Science* **2011**, *334*, 965.
[21] T. Liu, B. M. Zhao, J. W. Zhang, *Polymer* **2020**, *194*, 122392.
[22] J. C. Salamone, C. C. Tsai, A. P. Olson, A. C. Watterson, *J. Polym. Sci. A Polym. Chem.* **1980**, *18*, 2983.
[23] J. C. Salamone, N. A. Mahmud, M. U. Mahmud, T. Nagabhushanam, A. C. Watterson, *Polymer* **1982**, *23*, 843.
[24] S. Jana, V. A. Vasantha, L. P. Stubbs, A. Parthiban, J. G. Vancso, *J. Polym. Sci. A Polym. Chem.* **2013**, *51*, 3260.
[25] G. D. Deng, K. A. Cavicchi, *Macromolecules* **2017**, *50*, 9473.
[26] A. Eisenberg, J.-S. Kim, *Introduction to Ionomers*, Wiley, New York, USA, **1998**.
[27] M. Tolinski, *Additives for Polyolefins*, Elsevier, Oxford, UK, **2015**.
[28] J. Vachon, P. Neuteboom, J. Tellers, Patent WO 2021009274 **2020**.
[29] R. W. Rees, D. J. Vaughan, *ACS Polym. Preprints* **1965**, *6*, 287.
[30] R. W. Rees, *US Patent* 3,264,272, 1966.
[31] L. Cortes, F. Li, J. Tippet, K. Blackmon, M. Myhall, L. Daniels, J. Ashbaugh, *Patent WO 2016114802* **2015**.
[32] S. R. Gaikwad, S. J. S. Deshmukh, R. G. Gonnade, P. R. Rajamohanan, S. H. Chikkali, *ACS Macro Lett.* **2015**, *4*, 933.
[33] W. Zhao, Z. H. Liu, Y. A. Zhao, Y. Luo, S. B. He, *Inorganics* **2022**, *10*, 26.
[34] P. I. Nagy, P. W. Erhardt, *J. Phys. Chem. B* **2012**, *116*, 5425.
[35] C. Houriez, V. Vallet, F. Réal, M. Meot-Ner, M. Masella, *J. Chem. Phys.* **2017**, *147*, 161720.
[36] I. V. Fedorova, L. P. Safonova, *J. Phys. Chem. A* **2020**, *124*, 3170.
[37] H. Ghorbani, T. Christen, M. Carlen, E. Logakis, L. Herrmann, H. Hillborg, L. Petersson, J. Viertel, *IEEE Trans. Dielectr. Electr. Insul.* **2017**, *24*, 1485.
[38] W. Choo, G. Chen, S. G. Swingler, *Proc. IEEE Int. Conf. Solid Dielectr.*, IEEE, Germany, **2010**, 1.
[39] B. X. Du, C. L. Han, J. Li, Z. L. Li, *IEEE Trans. Dielectr. Electr. Insul.* **2020**, *27*, 418.
[40] Y. Ohki, T. Asada, Y. Umeshima, M. Ikeda, *Electr. Eng. Jpn.* **1997**, *120*, 9.
[41] M. E. Karlsson, X. D. Xu, H. Hillborg, V. Ström, M. S. Hedenqvist, F. Nilsson, R. T. Olsson, *RSC Adv.* **2020**, *10*, 4698.
[42] R. Kádár, M. Abbasi, R. Figuli, M. Rigdahl, M. Wilhelm, *Nanomaterials* **2017**, *7*, 23.